Report No. EMB-5

Copy No. 11

PRESSURE DISTRIBUTION AND FORCE COEFFICIENTS ON A 20° CONE USING EXPERIMENTAL AND THEORETICAL METHODS AT MACH NUMBER 1.93.

Prepared by W. H. Dorrance

Approved by J. Rutkowski

September 15, 1948

TABLE OF CONTENTS

Introduction

Supersonic wind tunnel tests on various configurations are being conducted to provide basic aerodynamic data. Initially, a series of pressure survey tests are being run as a first part of a broad program. The first of the series of pressure distribution tests were made on a 20° included angle cone model at a Mach number of 1.93. These tests provide data for comparison evaluation of the wind tunnel test results on a simple model with that of other tunnels as well as with theoretical results.

Summary

Wind tunnel pressure tests were run on a 20° included angle cone at a Mach number of 1.93 and the results are compared with existing theory and test results of other organizations. On the basis of the test results the following conclusions are drawn:

1. The numerical integration method of Taylor and Maccoll tabulated in Reference 1 gives value of drag coefficient slightly lower in magnitude than actually occurs. However, the difference in magnitude between experiment and theory is not significant.
2. The linearized theory gives reasonably correct values of pressure coefficient at zero angle of attack for the 20° cone.
3. These tests indicate that conical flow may not be preserved at angles of attack as is assumed by the linearized theories of Tsien and Von Karman and Moore. However, at small angles of attack the departure of the flow field from the conical condition is slight.
4. The approximate method advanced by Reference 3 will give values of drag coefficient fairly correct in magnitude but will predict a lift coefficient higher than that which actually occurs due mostly to the assumption of conical flow at angles of attack, and the omission of viscosity effects.
5. The data determined by these tests quantitatively checks with the results of tests run by other organizations and in most cases shows better test accuracy.

This report presents curves of pressure coefficients, lift coefficients, drag coefficients and center of pressure versus angle of attack for 20° cone as calculated from pressure data obtained from wind tunnel tests.

Symbols

A = frontal area of model

A_b = area of base of model

C_D = $\frac{DRAG}{q_o A}$ = drag coefficient

C_{D_b} = $\frac{(P_b - P_o)}{q_o} \times \frac{A_b}{A}$

C_p = $\frac{P_s - P_o}{q_o}$ = pressure coefficient

C_L = $\frac{LIFT}{q_o A}$ = lift coefficient

C.P. = center of pressure

l = length of cone model

M = Mach number

P_b = base static pressure

P_o = free stream static pressure

P_s = cone surface static pressure

q_o = free stream dynamic pressure

x = axial station measured from tip of cone

I, II, III, IV and V = numerals indicating meridian planes at 0^o, 45^o, 90^o, 135^o and 180^o respectively

clockwise?

Discussion

The model used in the wind tunnel is shown in plan view in Figure 1. It is a 20° stainless steel cone equipped with 18 pressure orifices .0225" in diameter. The copper orifice tubing leading through the sting and supporting sector is .04" outside diameter and .022" inside diameter. The model is hand finished to as smooth a finish as possible.

Seventeen of the orifices supplied useful data - one orifice was plugged and could not be cleared. Readings were taken at angles of attack of approximately 0°, ± 2°, ± 4°, ± 6°, ± 8°, ± 10°, the model rotated 180°, and readings taken at approximately 0°, ± 4°, and ± 8° to check the symmetry of results. All runs were made at a Mach number of 1.93.

A Schlieren photograph was taken of each run. A plumb line was used to create a vertical reference line which appears in each Schlieren photograph. The actual angle of attack was read from these photographs. A typical schlieren photograph showing the model at approximately + 10° angle of attack is shown as Figure 2.

Two photographs of the manometer bank were also taken for each angle of attack. These photographs record the pressure data which is reduced to give the pressure distribution over the surface of the model. A typical manometer bank photograph giving the reading at + 10° appears in Figure 2. The first three fluid levels of five tube groups represent orifice meridian planes I, IV, and III respectively. The last level of three tubes represents base pressure orifices.

The theoretical methods used to determine the pressure distribution at zero angle of attack are those of the numerical integration method of Taylor and Maccoll in Reference 1 and the linearized method of Reference 2. As is reasonable to expect, the comparison between experiments and theoretical

results is fairly close considering the fact that the Taylor and Maccoll theory neglects viscosity and the linearized theory neglects both viscosity and the occurance of a finite shock wave.

The results of an approximation method given in Reference 3 was used to compare with experimental results at angles of attack. The comparison shows fair agreement between the lift and drag coefficients. This method also neglects viscosity which has its effect on pressure distribution through increasing the effective included cone angle. This method also assumes conical flow.

Figure 4 shows pressure coefficient plotted versus axial station for every meridian plane at zero angle of attack. The theoretical results and experimental results compare favorably when consideration is made of the following factors contributing towards any deviation:

1. No account of the boundary layer or viscous effects is taken by the theoretical calculations. The boundary layer tends to increase the effective cone angle.
2. The linearized method takes no account of either viscosity or a finite shock wave. This theory gives reasonable results for small cone angles only.
3. The numerical integration values as tabulated in Reference 1 were extrapolated to give values at Mach number 1.93. This leads to a slight error in results.
4. Although extreme care was taken in fabricating the model, some deviations will occur in the geometry of the model with a corresponding effect on pressure readings.
5. Some test section velocity fluctuation is unavoidable which contributes slightly to inaccuracies in experimental results.

6. The method employed to set the angles of attack was not an accurate one. Reading the angle from a photograph gives limited accuracy.
7. Some undetected roll and yaw of the model may have occured while the runs were being made. This leads to errors in the pressure readings.

The experimental results plotted in Figure 4 agree with the theory of existance of a conical flow field at zero angle of attack. This is substantiated by the existance within experimental accuracy of a constant pressure coefficient for each meridian plane over the surface at zero angle of attack. References 4 and 5 reported similar results for slightly lower Mach numbers.

Figures 5, 6, 7, 8 and 9 present plots of pressure coefficient versus axial distance for five meridian planes at angles of attack of $\pm 2^{\circ}$, $\pm 4^{\circ}$, $\pm 6^{\circ}$, $\pm 8^{\circ}$, and $\pm 10^{\circ}$. The experimental points are connected by a solid line while the mean values of pressure coefficient for each meridian plane are represented by a straight broken line.

Figures 5 and 6 for $\pm 2^{\circ}$ and $\pm 4^{\circ}$ shows that within experimental accuracy the pressure coefficients for each axial station of a meridian plane does not deviate very much from a constant value. This indicates that the flow field has not departed far from conical flow at these small angles. Since the linearized theory presumes the conical field to be preserved at small angles of attack the theoretical results of the linearized theory and experiment should be fairly close. The method outlined in Reference 3 also assumes the conical field to be preserved at small angles of attack, and it will be shown later that results of this method compare favorably with test results.

The lines in Figures 5, 6, 7, 8 and 9 representing a constant mean pressure coefficient for each meridian plane were used in the graphical integration determining the lift, drag and moment of the model. This procedure employing a constant pressure coefficient for each meridian plane was adopted because it was shown that at the small angles of attack (2° and 4°) this condition approximately existed and for the higher angles the deviation from this condition was not much more than the accuracy limits of test data. It is thought that the calculations based on this assumption will yield nearly correct values of lift and drag coefficient while the error in moment will increase as angle of attack increases.

Figures 7, 8, and 9 showing pressure coefficient for $\pm 6^\circ$, $\pm 8^\circ$ and $\pm 10^\circ$ tend to indicate that at these angles the conical flow field no longer exists. No trend in pressure coefficient along a meridian plane seems to exist other than the fact that it seems to be highest in the region of the tip. Tests reported in References 4 and 5 also found this type of behavior in pressure coefficient although the scatter of test points was much greater because of more deviations of test conditions. It is seen, however, that the values of pressure coefficient do not depart far from a mean value at angles of attack as high as 10° which indicates that the flow field has not departed very far from a conical flow field.

It can be seen that the pressure coefficients representing meridian plane II at 45° are less than those representing meridian plane I at 0°. This somewhat startling result was not found in the tests reported by References 4 and 5 and may be explained by the possibility of some roll and yaw of the model being present at the time of these runs. The tests for plane I were run with the model at positive angles of attack while those of plane II were run at negative angles. If the model was not symmetrically aligned with the stream the behavior as shown in Figures

5, 6, and 7 may conceivably have occurred. However, it is difficult to explain why the pressure should be lower at plane II than at plane I at positive angles of attack unless some other flow deviation occurred. It is thought that this manifestation is an additional indication of the departure of the flow field from exact conical flow conditions.

Figure 10 gives values of drag and lift coefficient versus angle of attack. The value of drag coefficient determined experimentally compares favorably in magnitude and trend with those values determined with the approximation method of Reference 3 and with the magnitude of the numerical integration method of Reference 2. Reference 2 considers the value of the drag coefficient as being constant for small angles of attack. Experiment showed that drag coefficient was approximately constant up to 4° angle of attack which is the region considered by Reference 2. The experimental drag coefficient is higher than theoretical because of the omission by the theory of consideration of the effects of viscosity.

Lift coefficients shown in Figure 10 were somewhat lower than theory as was to be expected. The deviation from theory was greater at higher angles where the viscous effects not considered by theory begin to take a greater effect on the pressure distribution. However, the slope of the lift curve was shown to remain constant as is predicted by theory.

The location of the center of pressure is presented in Figure 11. These values were determined by making use of the moment calculations using the constant mean pressure coefficients. These values are not correct in magnitude because of this approximation and are only indicative of the trend of center of pressure location. The theoretical constant location predicted by the linearized theory is shown to be in error by this data.

The value of base drag coefficient for zero angle of attack was calculated by using the value of base pressure registered by the orifices on the base of the model. This experimental value compared favorably with values reported in Reference 10 found for tests run under similar conditions at a slightly lower Mach number but at the same Reynolds number. (Since the base pressure is largely affected by the boundary layer condition over the model which in turn is a function of the Reynolds number these values should compare favorably even though the Mach number differs slightly.) The two values are shown below.

	Cone Test	Reference 10
C_{D_b}	.152	.14 to .16

This result serves to indicate that probably very little deviation from normal test conditions occurred during the cone tests.

SKETCH OF 20° INCLUDED ANGLE CONE MODEL SHOWING ORIFICE STATIONS AND NUMBERING

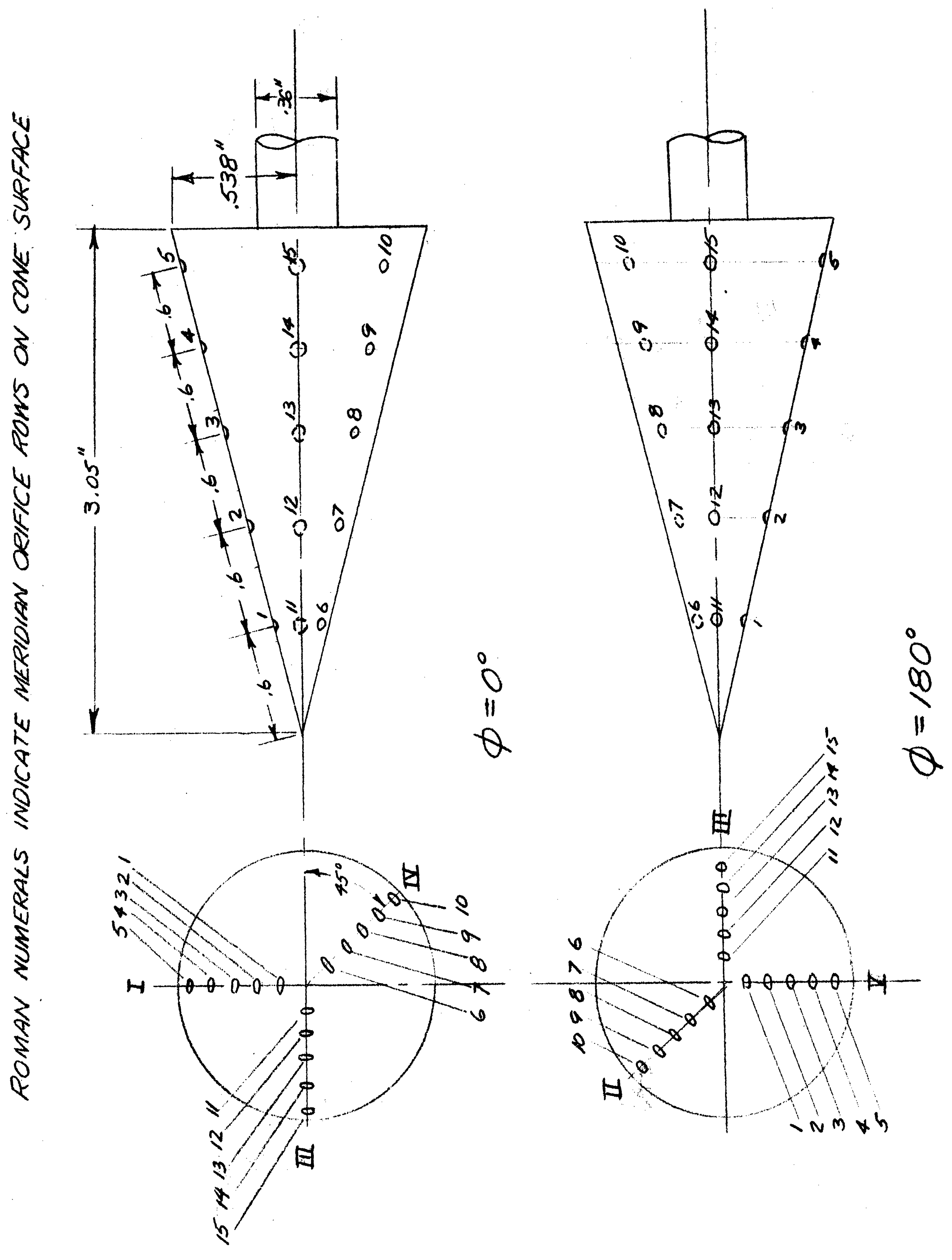

FIGURE 1

PRESSURE COEFFICIENT VS AXIAL STATION FOR THE 20° CONE AT M=1.93 $\alpha = 0°$ ALL STATIONS HAVE IDENTICAL VALUE OF C_p

⊙ DENOTES EXPERIMENTAL VALUES

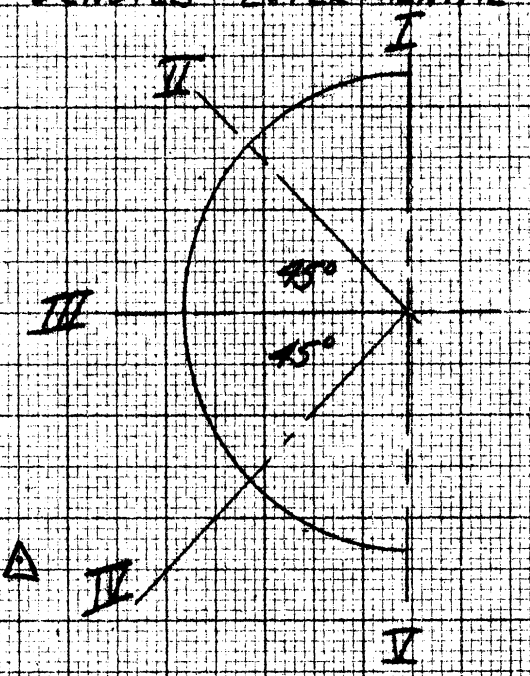

MERIDIAN PLANES REPRESENTED BY TEST DATA

Δ Experimental points by Taylor and Maccoll on 20° Cone at 2.09 M

PRESSURE COEFFICIENT $-C_p$

.15
.14
.13
.12
.11
.10
.09
.08

WIND TUNNEL DATA ⊙ M=1.93

SAUER'S LINGARIZED METHOD M=2.0

Δ TAYLOR-MACCOLL M=1.95 (EXTRAPOLATED)

0 .1 .2 .3 .4 .5 .6 .7 .8 .9 1.0

AXIAL DISTANCE $\frac{x}{l}$

FIGURE 4

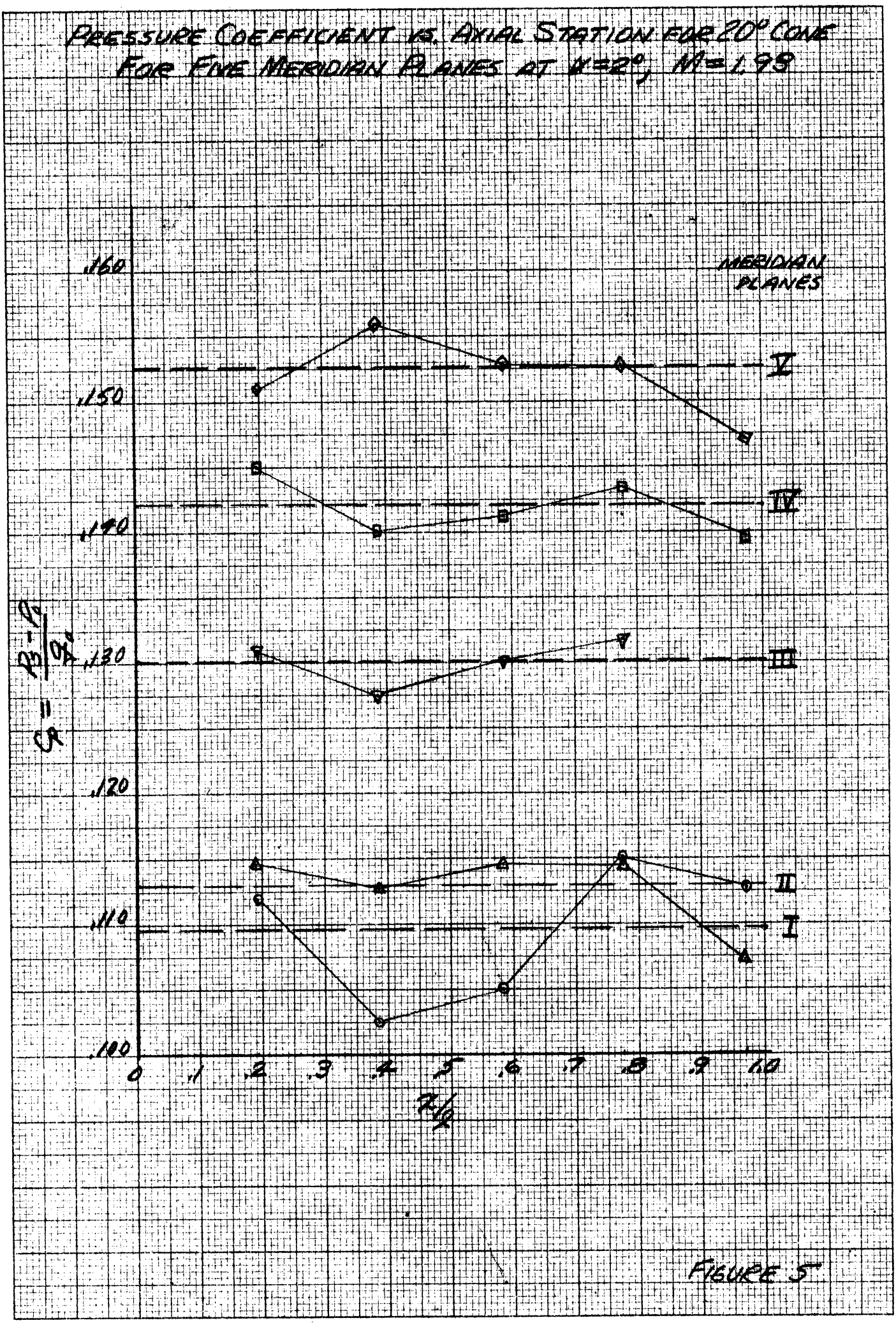

FIGURE 5

PRESSURE COEFFICIENT VERSUS AXIAL STATION FOR 20° CONE FOR FIVE MERIDIAN PLANES AT $\alpha = 4°$, $M = 1.93$

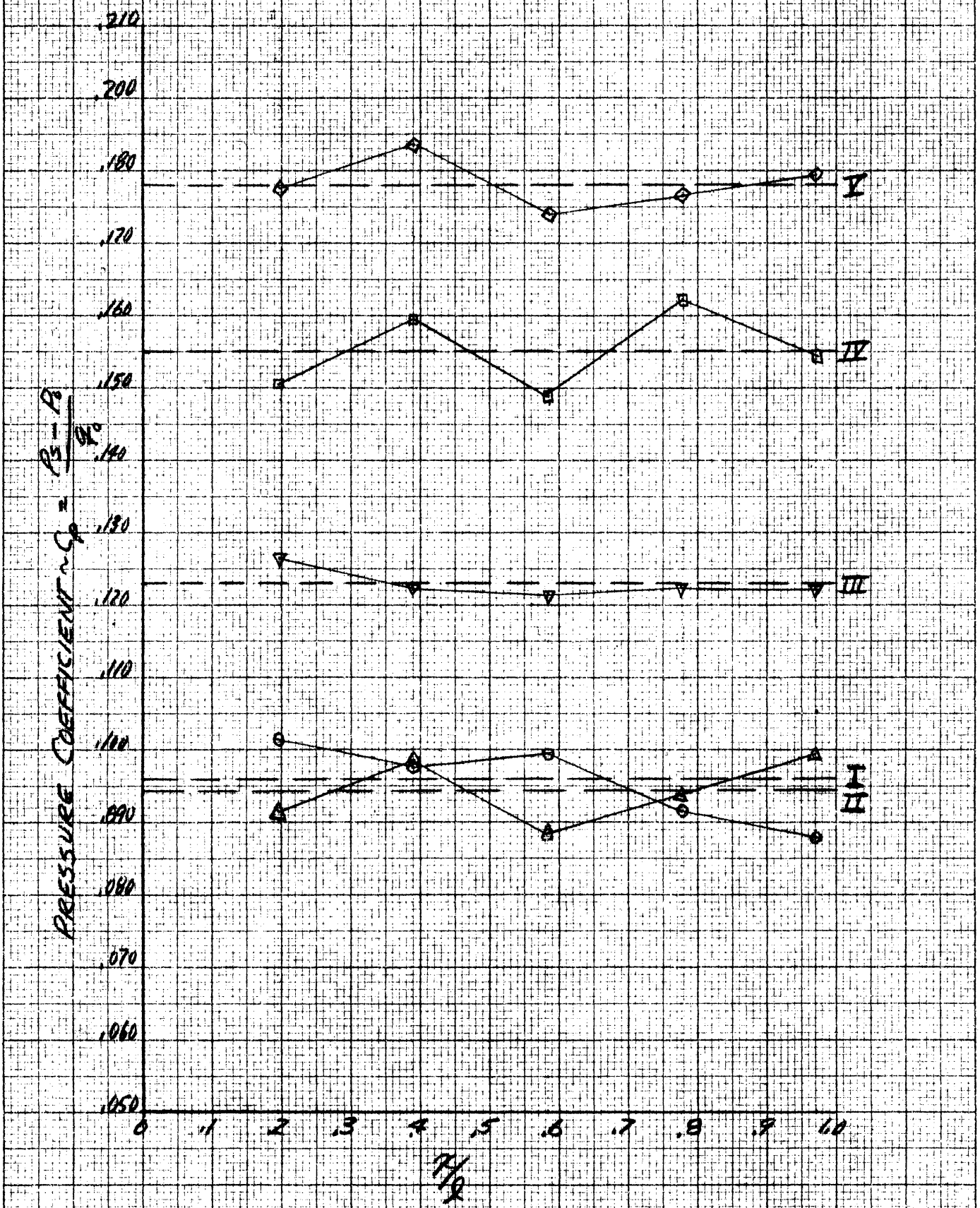

FIGURE 6

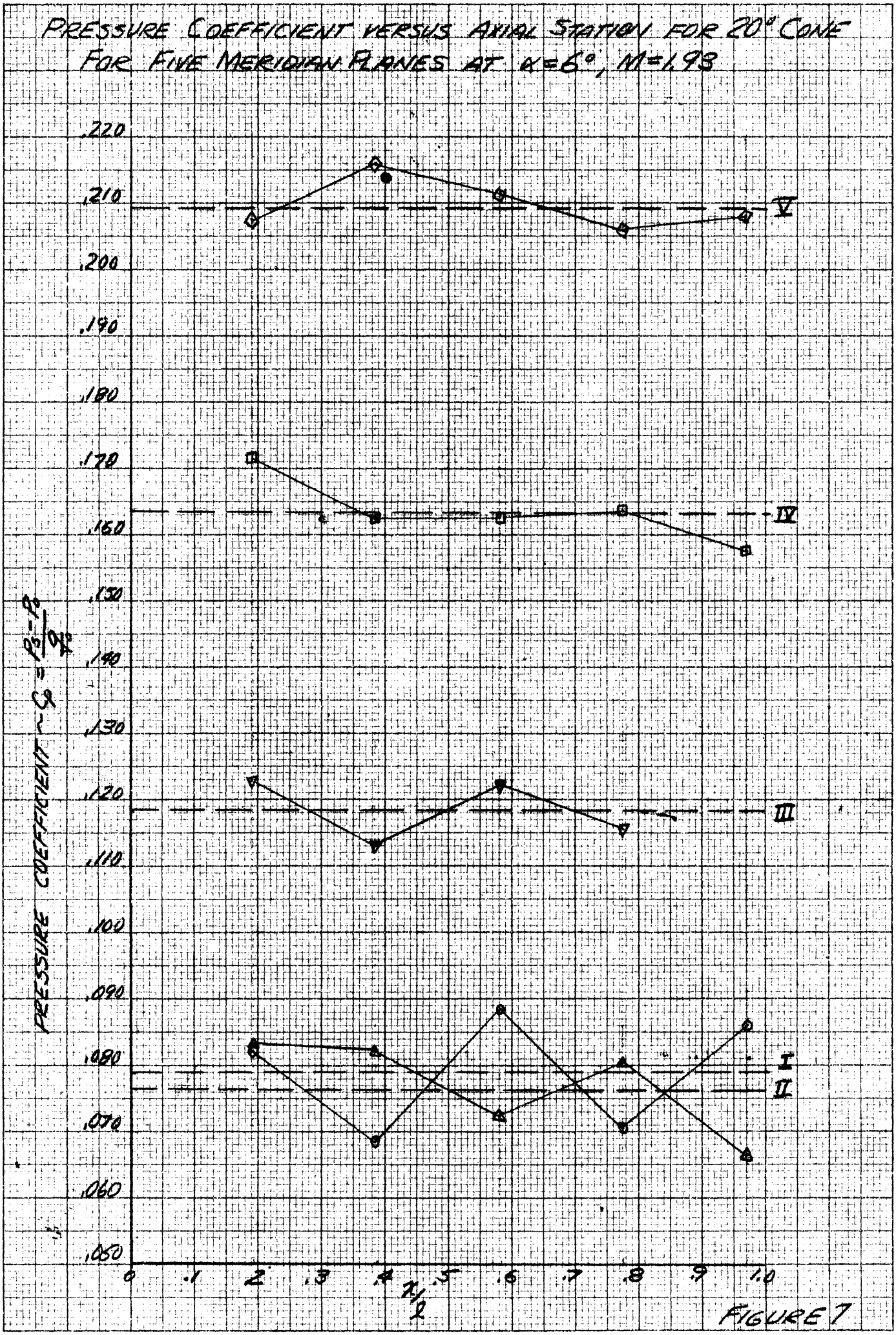
PRESSURE COEFFICIENT VERSUS AXIAL STATION FOR 20° CONE
FOR FIVE MERIDIAN PLANES AT α=6°, M=1.98
PRESSURE COEFFICIENT - $C_p = \frac{p_s - p_\infty}{q_\infty}$
.220
.210
.200
.190
.180
.170
.160
.150
.140
.130
.120
.110
.100
.090
.080
.070
.060
.050
0
.1
.2
.3
.4
.5
.6
.7
.8
.9
1.0
$\frac{x}{l}$
V
IV
III
I
II

FIGURE 7

PRESSURE COEFFICIENT VS. AXIAL STATION FOR 20° CONE FOR FIVE MERIDIAN PLANES AT $\alpha = 8°$, $M = 1.93$

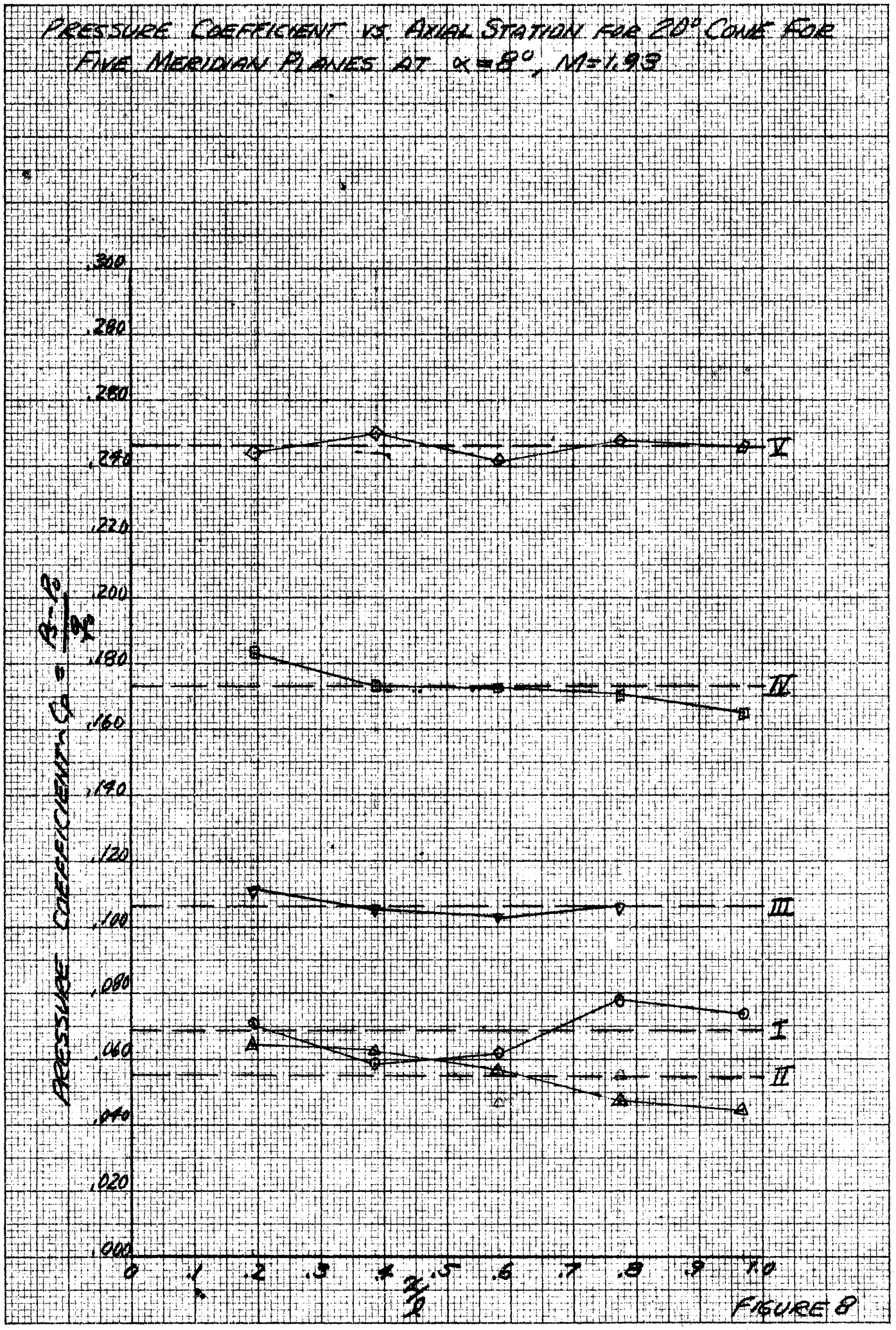

FIGURE 8

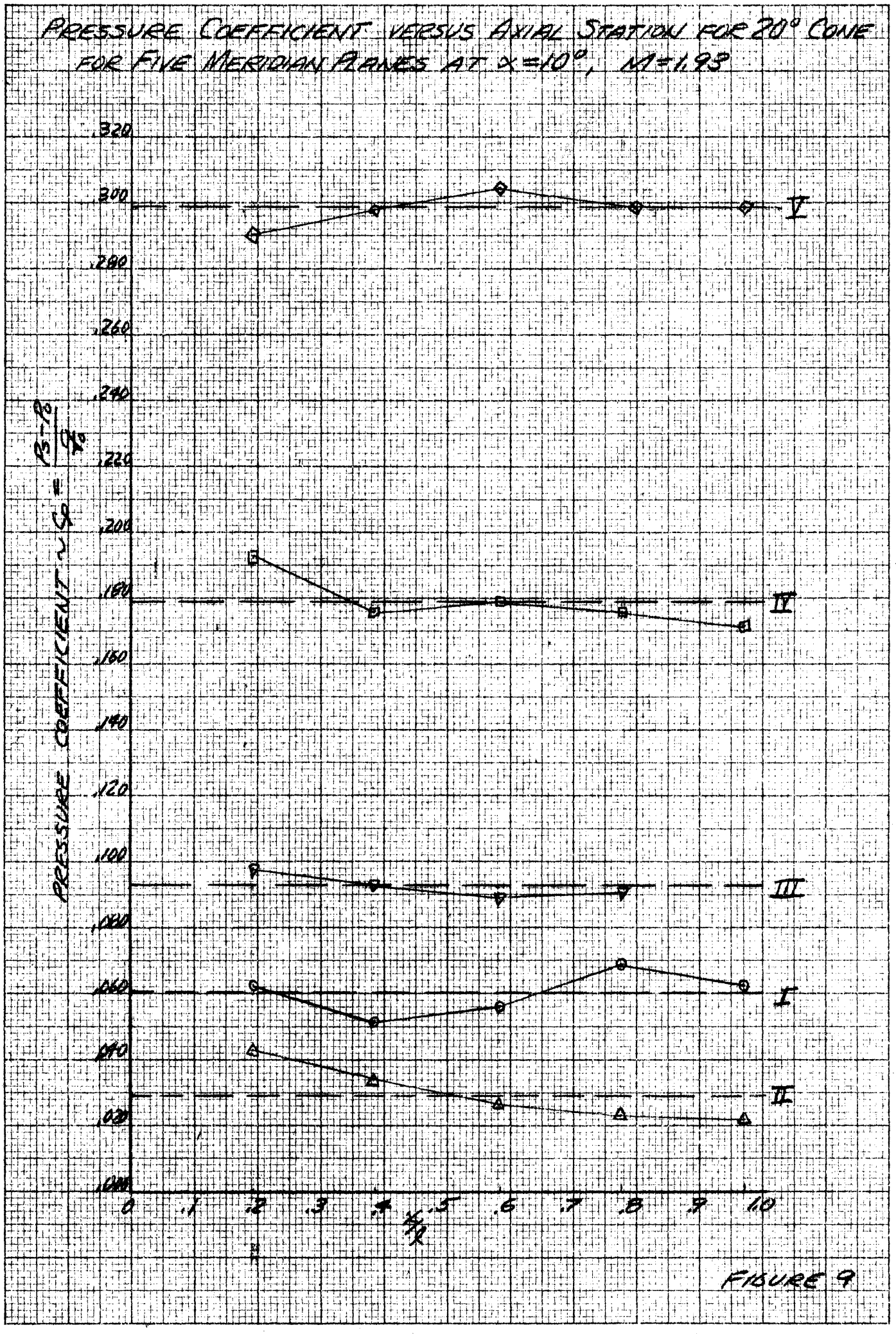
PRESSURE COEFFICIENT VERSUS AXIAL STATION FOR 20° CONE
FOR FIVE MERIDIAN PLANES AT α=10°, M=1.93
PRESSURE COEFFICIENT = (p-p0)/q0
.320
.300
.280
.260
.240
.220
.200
.180
.160
.140
.120
.100
.080
.060
.040
.020
.000
0
.1
.2
.3
.4
.5
.6
.7
.8
.9
1.0
x/R
V
IV
III
I
II

FIGURE 9

DRAG COEFFICIENT VS. ANGLE OF ATTACK FOR 20° CONE MODEL

— — — — — REF: M.I.T.-UAC-3
REF: MIT-TR-3

M=1.93

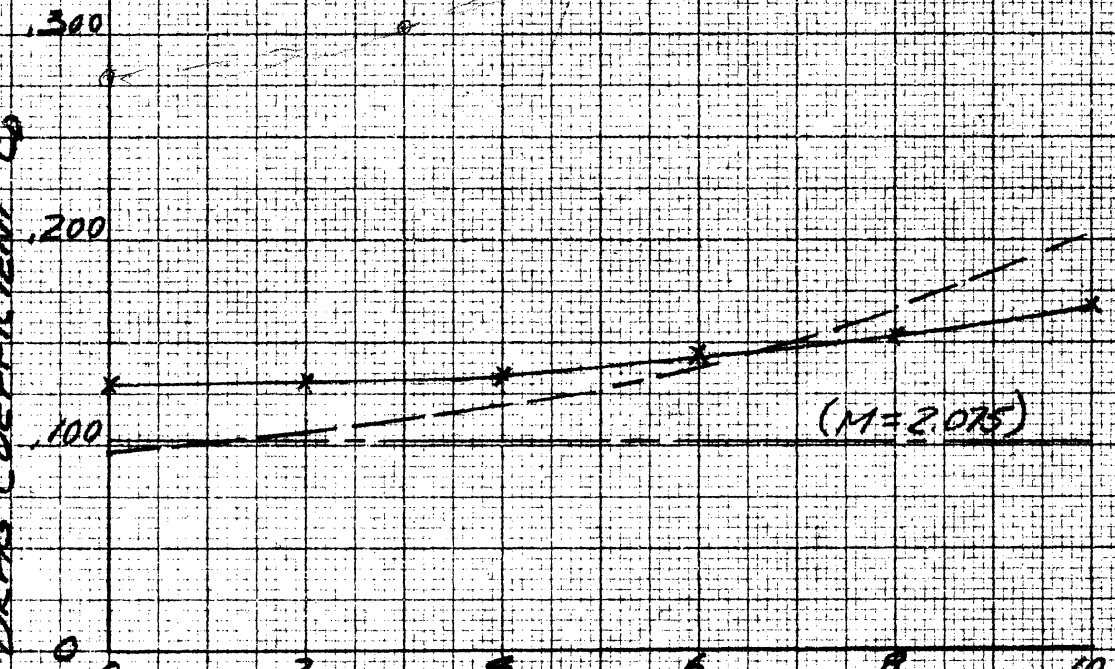

LIFT COEFFICIENT VS. ANGLE OF ATTACK FOR 20° CONE MODEL

— — — — REF: MIT-UAC-3

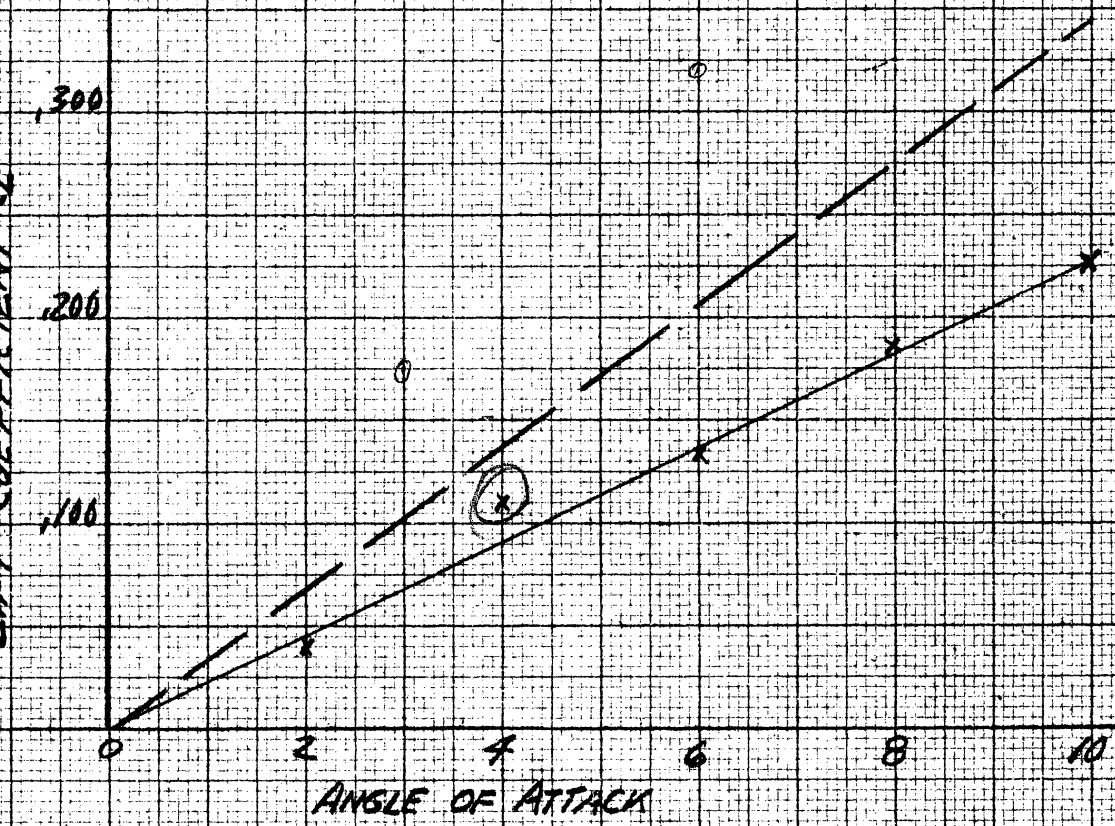

FIGURE 10

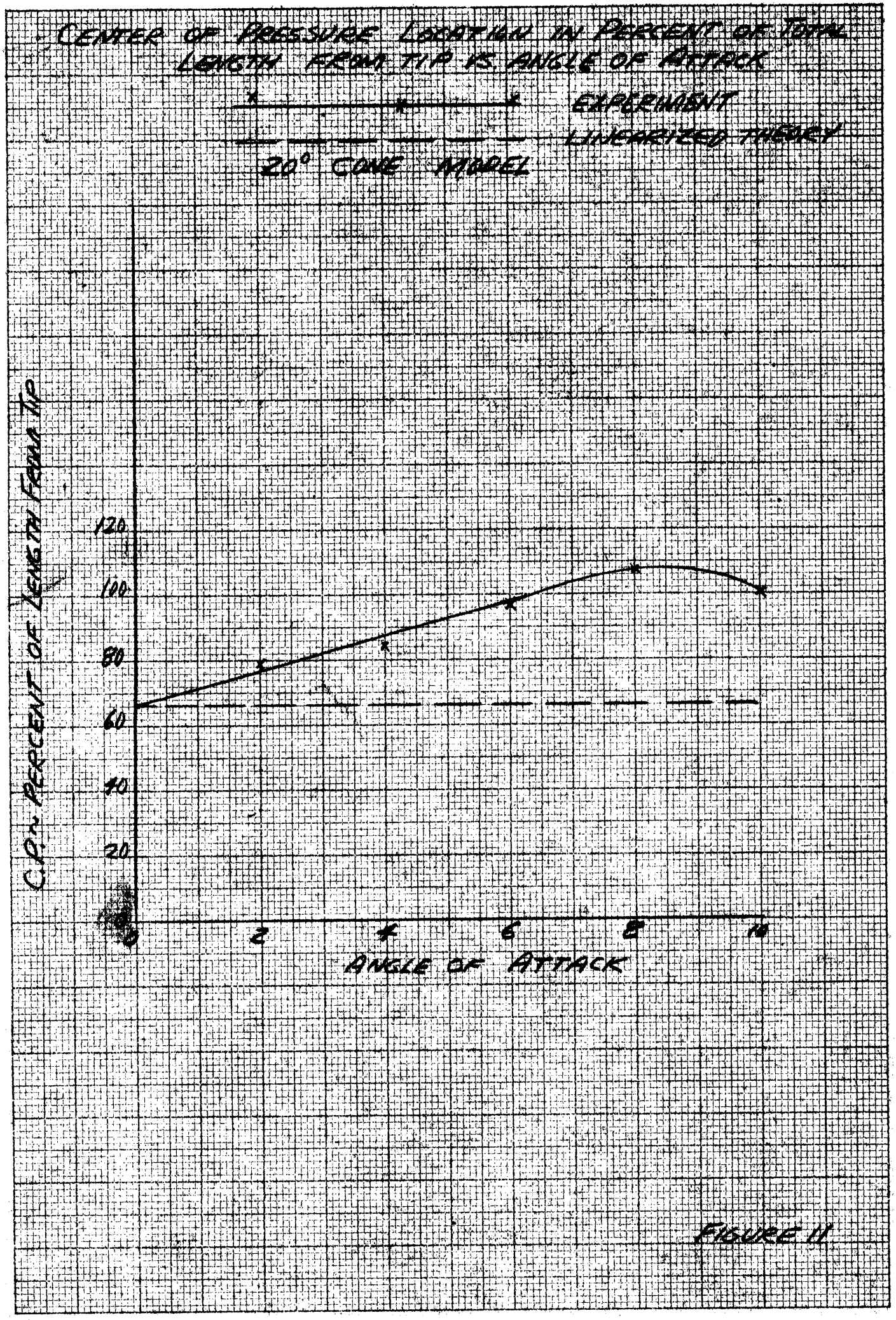

FIGURE 11

References

1. "Supersonic Flow of Air Around Cones", MIT-TR-1.

2. "Linearized Supersonic Flow Around Yawed Bodies of Revolution", By R. Sauer, Curtiss-Wright Corporation, Translation CGD-620.

3. "Method of Determining Lift, Drag and Pitching Moment of Inclined Cones at Supersonic Speeds", MIT-Meteor-UAC-3.

4. "Pressure Survey on Cones in the Two-Dimensional, 1.73 M, Free Jet at F.G.S.", Applied Physics Laboratory, Johns Hopkins University CF-716-N.

5. "Experimental Determination of Pressure on the Surface of a Cone in a Supersonic Stream", Applied Physics Laboratory, Johns Hopkins University CF-530-N.

6. "Air Pressure on a Cone Moving at High Speeds", By G. I. Taylor and J. W. Maccoll.

7. "Resistance of Slender Bodies Moving with Supersonic Velocities with Special Reference to Projectiles", by Theodore Von Karman and Norton B. Moore, American Society of Mechanical Engineers, June 1932.

8. "Supersonic Flow Around Yawing Cones", MIT-TR-3

9. "Supersonic Flow of an Inclined Body of Revolution", by H. S. Tsien, Journal of Aeronautical Science, Volume 5, 1937.

10. "Experimental Investigation of the Effects of Support Interference of the Drag of Bodies of Revolution at a Mach Number of 1.5", National Advisory Committee on Aeronautics RM A8B05.

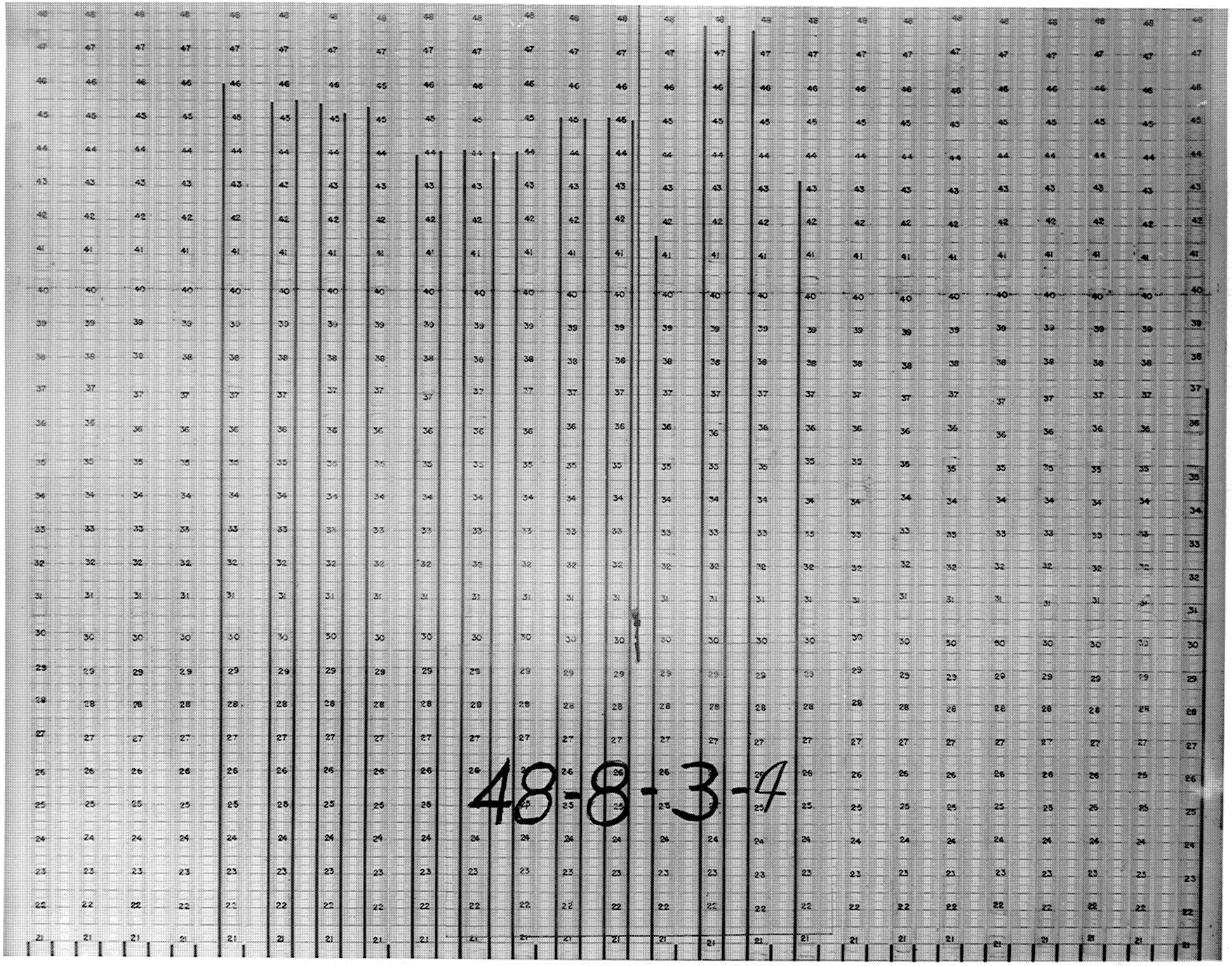
48-8-3-4

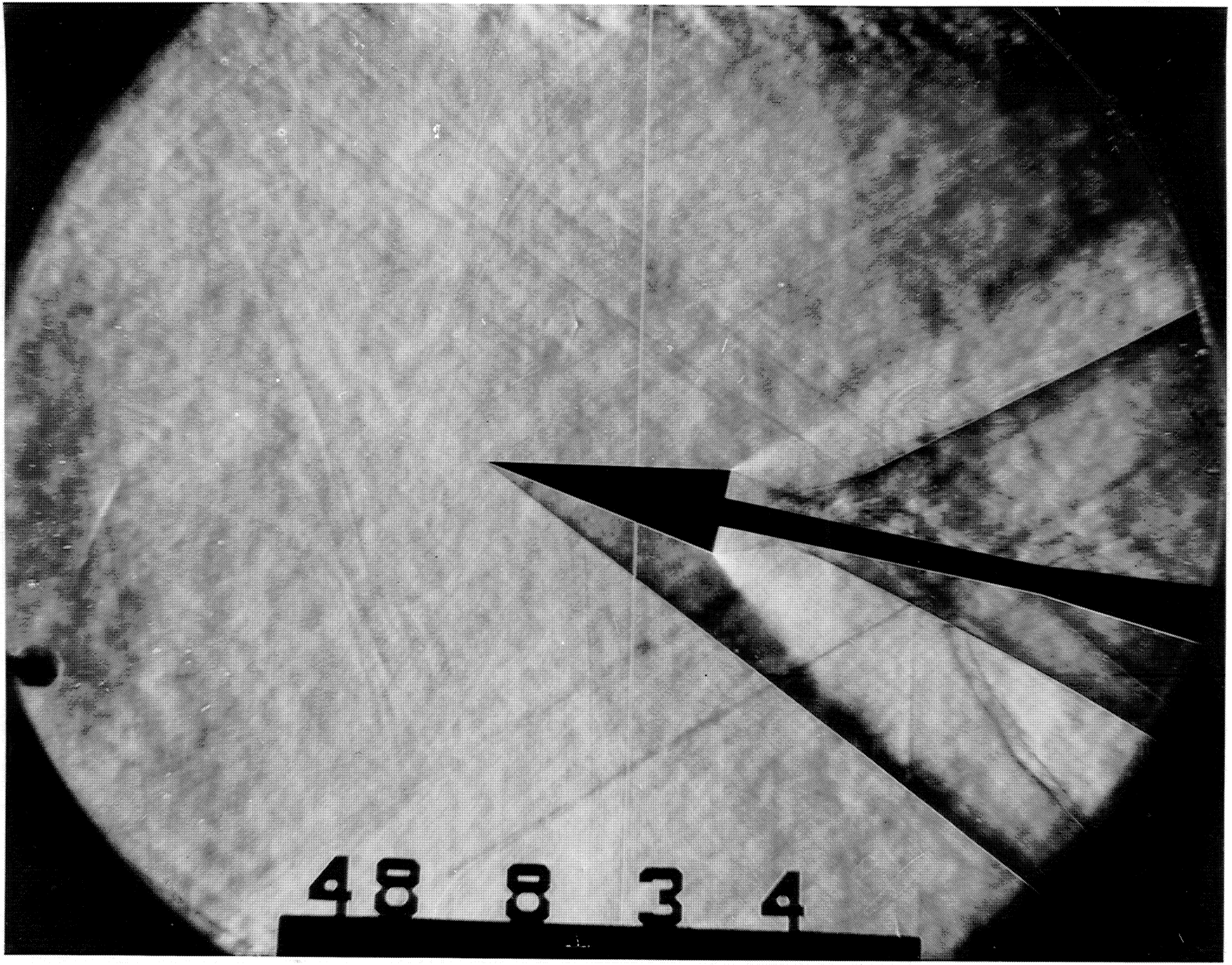
4 8 8 3 4